

Temperature-dependent fracture toughness of Utah FORGE granite from semi-circular bending (SCB) tests: dataset and methods report

N. Z. Dvory¹  and J. D. McLennan² 

February 2026

1 Civil and Environmental Engineering and Energy & Geoscience Institute, University of Utah, Salt Lake City, UT, USA

2 Chemical Engineering and Energy & Geoscience Institute, University of Utah, Salt Lake City, UT, USA

Keywords: fracture toughness, SCB/NSCB, geothermal, Utah FORGE, temperature, LEFM, FPZ

1. Executive Summary

This report documents a fracture-toughness (FT) dataset developed to support geothermal stimulation proposals and to enable public reuse through the Geothermal Data Repository (GDR). The focus is on Mode-I fracture toughness, K_{IC} , measured on Utah FORGE core material using the semi-circular bending (SCB) method (ISRM Suggested Method), with emphasis on at-temperature (“real-time”) testing rather than post-heating/cooled protocols.

Dataset scope

- **Lithology/site:** Utah FORGE field laboratory samples (granitic lithology emphasized). Ambient-temperature results are reported for multiple rock units from **Well 58-32** (including granitic and related crystalline units).
- **Depths represented:** The high-temperature trend figure highlights a granite sample set retrieved from **~5,874 ft** depth, plus a shallower granite data point used as a comparison.
- **Temperature range:** High-temperature SCB testing is described as controlled from **~25°C to 250°C** in the current setup, with motivation to extend coverage to higher geothermal-relevant temperatures in future work.

Main outcome

The dataset indicates a non-monotonic $K_{IC}(T)$ behavior in FORGE granite:

- **Moderate-temperature toughening** (interpreted as closure of pre-existing microcracks due to thermal expansion), followed by
- **Toughness degradation beyond a critical temperature T_{crit}** (interpreted as the onset and accumulation of thermal microcracking and related microstructural weakening).

The report also documents an important quality-control exception: at 100°C, one specimen did not initiate at the intended notch tip and failed at a lower load, consistent with failure along a pre-existing natural fracture rather than the induced crack tip. This case should be flagged in the released dataset.

Primary use cases

1. Stimulation design and operational planning

Incorporate temperature-dependent toughness into expectations for fracture initiation/propagation sensitivity and stress-shadow interactions in EGS-style treatments, especially where toughness-dominated behavior is expected.

2. Thermo-mechanical and coupled fracture modeling

Provide calibration targets for models that include temperature-dependent fracture resistance and that distinguish “at-temperature” response from cooled, thermally damaged response.

2. Scientific Background and Motivation

2.1 Geothermal relevance

Fracture propagation is a primary mechanism by which stimulation creates and sustains the hydraulically connected surface area required for heat extraction. In Enhanced Geothermal Systems (EGS), injectivity and long-term thermal performance depend on whether stimulation produces a distributed fracture network (favorable for conforming fluid distribution and heat exchange) or concentrates slip and opening on a limited set of structures (which can reduce sweep efficiency and increase operational risk). Because fracture growth modifies the stress field (stress shadow) and redistributes deformation between opening and shear, fracture propagation processes are inherently linked to both stimulation efficiency and induced-seismicity risk.

Fracture growth and associated slip also generate seismic and microseismic responses that are routinely used as operational diagnostics. These signals provide information on stimulated volume, fracture interaction, and proximity to critically stressed faults. The same processes that improve connectivity (opening, branching, coalescence) can also promote unstable slip when perturbations in stress and pore pressure activate pre-existing discontinuities. Therefore, the ability to predict fracture propagation thresholds is central to designing stimulation schedules (rate, pressure limits, stage spacing) that maximize permeability gains while managing the probability of runaway fracture growth and fault activation.

Temperature-dependent fracture toughness is particularly important for superhot/supercritical geothermal targets and high-temperature EGS environments, as temperature alters the rock's fracture resistance through competing mechanisms. At moderate temperatures, thermal expansion can partially close pre-existing microcracks, increasing apparent toughness. At higher temperatures, differential mineral expansion and thermochemical changes promote thermal microcracking, increasing damage and reducing toughness. The net result can be a non-monotonic $K_{IC}(T)$ response, with a toughness peak followed by a decline beyond a critical temperature. This behavior implies that, in hot reservoirs, relatively small changes in stress or pore pressure can shift fault growth from localized to more extensive propagation, increasing sensitivity to stress shadows and the likelihood of unintended connectivity or seismic activation.

From a modeling and design perspective, fracture toughness directly enters criteria for crack extension and regime selection in hydraulic fracturing (toughness-dominated versus viscosity-dominated behavior). Consequently, assuming a temperature-independent K_{IC} can bias predictions of fracture geometry, required injection pressures, and interaction distances between fractures (Dontsov and Suarez-Rivera, 2020a, 2020b; Dvory et al., 2025, 2024b, 2024a) (Figure 1). For superhot/supercritical settings—where temperatures may exceed the range of conventional geothermal operations—determining $K_{IC}(T)$ with in-situ-relevant testing is necessary to support credible stimulation forecasts, risk-informed operating envelopes, and mechanistically defensible scaling toward field-scale fracture simulations.

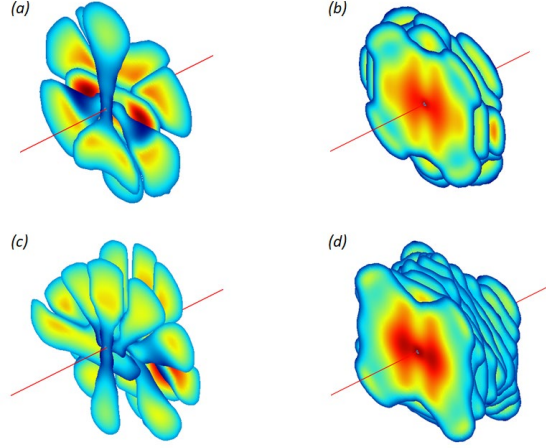


Figure 1: Hydraulic fracture geometries for closely spaced fractures generated in different regimes (Dontsov and Suarez-Rivera, 2020b). (a): Toughness dominated, 5 fractures. (b): Viscosity dominated, 5 fractures. (c): Toughness dominated, 10 fractures. (d): Viscosity dominated, 10 fractures.

2.2 Fracture mechanics framework

LEFM crack-growth criterion

Mode-I extensional crack growth is commonly described using Linear Elastic Fracture Mechanics (LEFM), where the crack-tip stress intensity factor K scales with loading and crack size, and fracture extension is expected when the applied intensity exceeds the material resistance (fracture toughness) (Anderson, 2017):

$$K = Y \sigma \sqrt{\pi a}, \quad K \geq K_{IC}. \quad (1)$$

Here, Y is a geometry factor, σ is the applied stress, and a is a characteristic crack length.

An equivalent statement uses energy balance (Griffith-type) in terms of the energy release rate G :

$$G = \frac{K^2}{E'}, \quad G \geq G_c, \quad (2)$$

where E' is the effective elastic modulus (plane stress/plane strain dependent), and G_c is the critical fracture energy (Anderson, 2017).

Thermal stress scaling and microcrack initiation

Elevated temperatures produce additional stresses due to the differential thermal expansion of mineral grains. A standard thermoelastic scaling under plane strain is (Jaeger et al., 2007; Timoshenko and Goodier, 1970):

$$\sigma_{th} = \frac{E \alpha \Delta T}{1-\nu}, \quad (3)$$

where E is Young's modulus, α is the coefficient of thermal expansion, ν is Poisson's ratio, and ΔT is the temperature increase.

Thermal microcracks can be conceived to initiate when thermoelastic stress reaches the tensile resistance (Jaeger et al., 2007; Timoshenko & Goodier, 1970):

$$|\sigma_{th}| \gtrsim |\sigma_t|, \quad (4)$$

with σ_t the tensile strength. This concept is consistent with observations that granitic rocks can develop pervasive thermal cracking above $\sim 200\text{--}300$ °C (Hu et al., 2022a; Sun et al., 2015).

Practical geothermal criterion (fluid pressure vs confinement vs toughness)

For geothermal stimulation and thermally influenced crack growth, a useful modeling form compares **internal fracture fluid pressure** to the opposing **normal stress** and the fracture resistance scale:

$$P_f - \sigma_3 \geq \frac{K_{IC}}{\sqrt{\pi a}}, \quad (5)$$

where P_f is internal fluid pressure, σ_3 is total normal (lithostatic/tectonic) stress, and a is a characteristic crack length. This provides an interpretable bridge between operational pressure margins and temperature-dependent toughness, which is the key parameter targeted by the SCB dataset for geothermal applications.

2.3 Expected temperature trends and competing mechanisms (no modeling)

Competing mechanisms controlling $K_{IC}(T)$

Mode-I fracture toughness can vary non-monotonically with temperature because two microstructural processes compete (Figure 2).

- (i) **Low–moderate temperature: apparent toughening by microcrack closure**
At modest temperature increases, differential thermal expansion of mineral grains can promote partial closure of pre-existing microcracks, increase contact across grain boundaries, and inhibit microcrack growth and coalescence. This mechanism is commonly cited to explain an initial increase in measured fracture toughness at moderate temperatures (Justo et al., 2020; Mahanta et al., 2016; Yin et al., 2012). One could also speculate that the process zone increases in size, and this effectively blunts the crack.
- (ii) **Higher temperature: toughness degradation by thermal microcracking and dehydration-related weakening**
As temperature increases further (often reported above $\sim 200^\circ\text{C}$ in granitic rocks), petrographic observations show the development of new thermal microcracks once thermoelastic mismatch stresses exceed intergranular/intragranular bond strengths (Hu et al., 2022). In addition, loss of bound/crystalline/structural water and related high-temperature changes can further weaken mechanical properties (Sun et al., 2015). These processes increase damage and reduce the resistance to crack extension, producing a post-peak decline in K_{IC} .

Implications for the fracture process zone (FPZ) and LEFM applicability

With increasing temperature and progressive damage, the fracture process zone (FPZ) ahead of the crack tip is expected to become more prominent, reflecting more distributed microcracking and dissipation. The

increased FPZ length, increased crack-tip opening, and more tortuous fracture surfaces as thermal effects intensify (e.g., Wang et al., 2025; Yin et al., 2020).

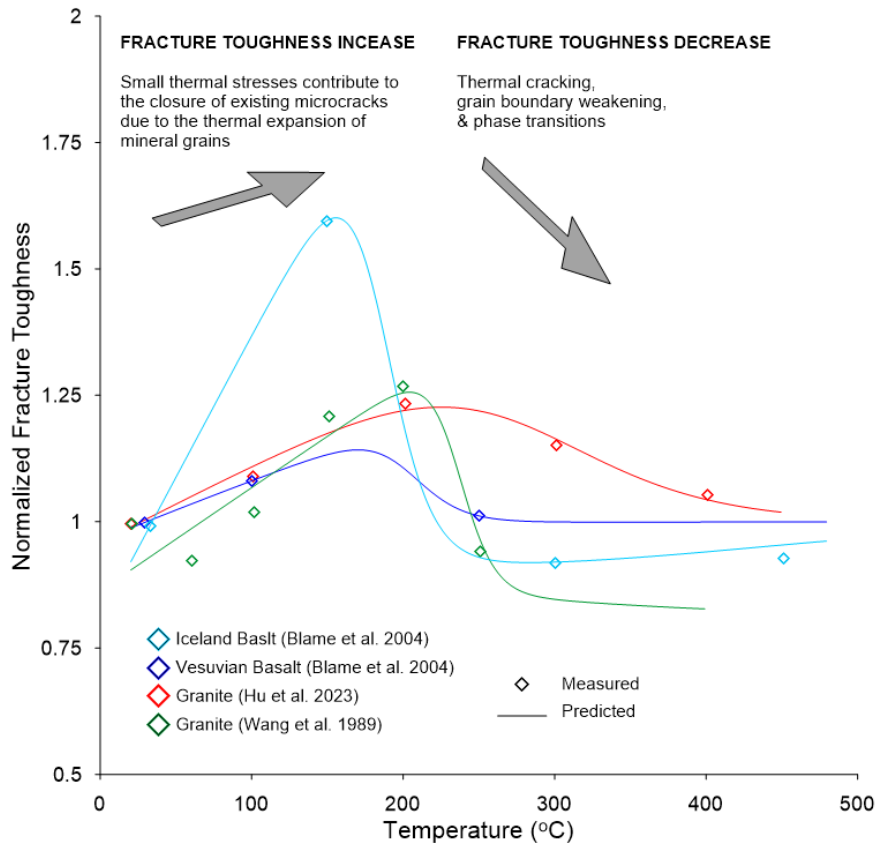


Figure 2: Relationship between fracture toughness and temperature of rock at high temperature in real-time (after Hu et al., 2024)

3. Objectives and Research Questions

This report aims to quantify the Mode-I fracture toughness of Utah FORGE granite as a function of temperature, $K_{IC}(T)$, using SCB tests conducted at elevated temperature (not post-heating/cooled specimens). The objectives are to document the observed non-monotonic trend (moderate-temperature increase followed by high-temperature decrease) and identify the approximate critical temperature T_{crit} marking the onset of degradation within the resolution of the testing protocols, and providing a transparent, reproducible workflow (geometry inputs, peak-load picking, validity criteria) with uncertainty bounds. In addition, the report summarizes the dataset with an empirical non-monotonic functional fit (e.g., Eq. 7) for compact representation and reuse. The associated research questions are:

- What is the measured $K_{IC}(T)$ trend for FORGE granite under-temperature loading;
- Is the non-monotonic behavior robust relative to specimen variability and QC-flagged off-notch failures; and,
- What temperature range indicates the transition to toughness degradation?

4. Experimental Methods

Mode-I fracture toughness was measured using semi-circular bending (SCB) tests on Utah FORGE core material, following the ISRM Suggested Method for SCB/NSCB fracture toughness determination

(Kuruppu et al., 2014) (Figure 3). Specimens were prepared from Utah FORGE core into semi-circular disks with a machined notch to define the Mode-I crack tip and then loaded in a three-point bending configuration to promote tensile opening at the notch tip. Load and displacement (or equivalent actuator/fixture displacement) were recorded continuously during monotonic loading to failure, and the peak load was combined with the appropriate SCB geometry factor to compute K_{IC} for each specimen.

To reduce bias associated with post-thermal-treatment testing, the campaign emphasized at-temperature (“real-time”) mechanical testing, in which specimens were heated to a target temperature and tested while maintained at that temperature (rather than cooled back to ambient). The temperature program covered the range accessible in the current setup (reported as approximately 25–250 °C) and was selected to probe the expected transition from moderate-temperature toughening to higher-temperature degradation. Temperature was monitored during heating and during the test window, and was stabilized before loading; these temperature-control details and sensor placement are documented in the repository metadata.

Quality control focused on verifying that fracture initiation occurred at the intended notch tip and that the observed failure mode was consistent with SCB assumptions. Tests exhibiting off-notch initiation were flagged; notably, a 100 °C specimen failed at lower load and did not initiate from the expected crack tip, interpreted as failure along a pre-existing natural fracture, and is treated as a QC exception in the dataset. Accordingly, fracture-toughness values are reported with specimen-level validity flags to distinguish notch-controlled failures from discontinuity-controlled failures.

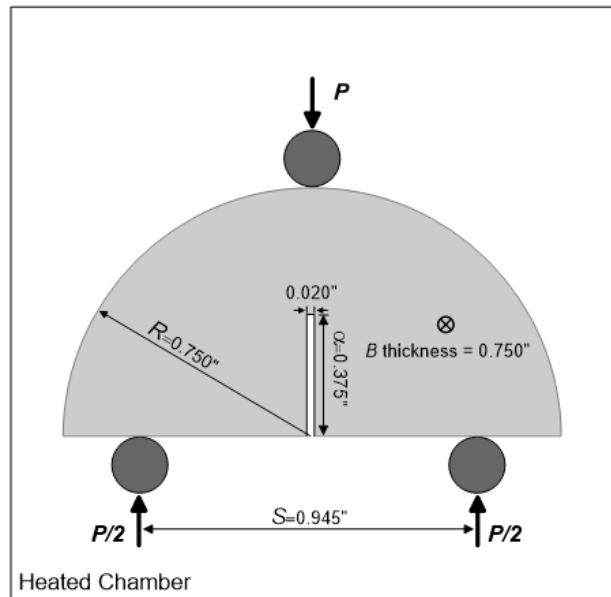


Figure 3: Experiment setups - Semi-circular bending (SCB) test with acoustic emission (AE) sensors.

5. Results & Discussion

We first report ambient-temperature values from Well 58-32 to establish a baseline across lithologies and sample orientations (Figure 4). We then present the at-temperature SCB results used to evaluate $K_{IC}(T)$.

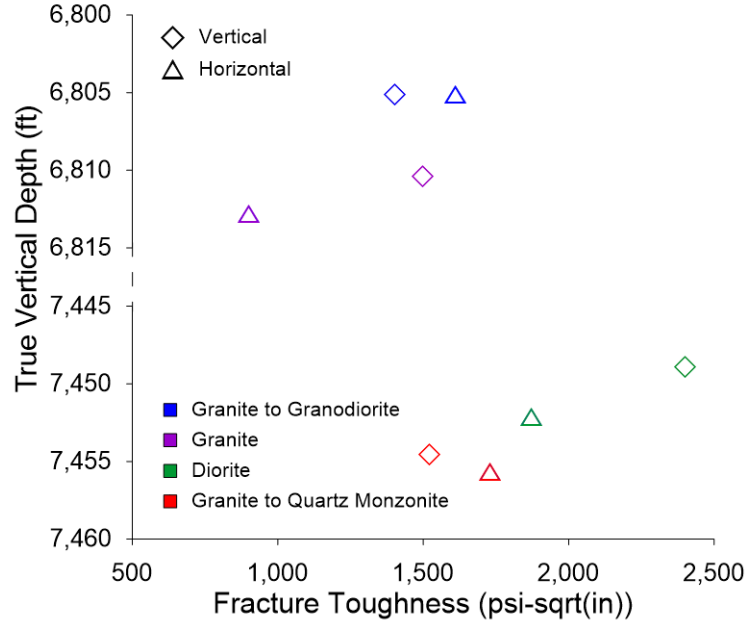


Figure 4: Results of fracture toughness experiments conducted at ambient temperature. The rock samples were extracted from cores taken from Well 58-32, located at the FORGE site.

Figure 5 shows an increase in the fracture toughness at moderate temperatures. With similarity to previous results shown in Figure 2, we suggest that the small thermal stresses contribute to the closure of existing microcracks due to the thermal expansion of mineral grains and thereby inhibit the propagation and interconnection of microcracks (Justo et al., 2020; Mahanta et al., 2016; Yin et al., 2012).

However, when the temperature exceeds about 200°C, petrographic thin-section analyses reveal the development of thermal microcracks in the granite (Hu et al., 2022). Figures 2 and 5 show that the measured Mode-I fracture toughness decreases as the temperature exceeds 200°C, primarily due to the accumulation of thermal microcracks. These microcracks form as thermal stress exceeds the minerals' intergranular and intragranular bond strength. Additionally, the loss of bound, crystalline, and structural water at elevated temperatures further weakens the mechanical properties of granite (Sun et al., 2015). The following general relationship can represent this behavior:

$$K_{IC}(T) = K_{IC}(T_0) \times f(T) \quad (6)$$

where $K_{IC}(T)$ is the fracture toughness at temperature T , $K_{IC}(T_0)$ is the room temperature toughness, and $f(T)$ describes a nonlinear temperature-dependency factor. This non-linear relationship reflects the cumulative effect of the rock's thermal expansion, microcrack formation, and mineralogical changes for the testing carried out. As temperatures increase, expansion-induced thermal stresses can cause pre-existing microcracks to grow and coalesce, accelerating crack propagation under stress. Hu et al. (2023) further suggest that the reduction in fracture toughness becomes more pronounced as critical temperature thresholds are reached, particularly in rocks with high quartz content, where phase transitions can drastically alter mechanical properties. In geothermal reservoirs, granitic or otherwise, where temperatures often exceed 300°C, the reduction in toughness could be substantial enough to affect fracture propagation, making the system more prone to mechanical failure or excessive crack growth.

This temperature sensitivity necessitates a more comprehensive understanding of fracture mechanics under geothermal conditions, where traditional assumptions about linear elastic fracture propagation may no longer hold.

The temperature-dependent behavior of fracture toughness invites a deeper exploration of fracture mechanics in geothermal reservoirs. The influence of temperature on fracture toughness affects fracture propagation and challenges the assumptions of conventional fracture propagation models, which often assume constant toughness. Dontsov & Suarez-Rivera (2020b) illustrated that fracture propagation is a dynamic process influenced by factors such as toughness, fluid viscosity, and stress interactions between fractures. Introducing temperature as a variable in this framework adds complexity and enhances the accuracy of predictive models to simulate geothermal reservoir behavior. In particular, the decrease in fracture toughness with temperature could lead to the development of extended fracture networks. This is especially significant in Enhanced Geothermal Systems (EGS), where fluid injections induce thermal and mechanical stresses that interact with pre-existing fractures. A reduced fracture toughness at elevated temperatures, and smaller perturbations in stress or temperature could initiate fracture extension, potentially leading to unintended fracture propagation and even induced seismicity. Understanding these mechanisms is vital for designing and managing geothermal reservoirs, where maintaining fracture stability is key to long-term performance.

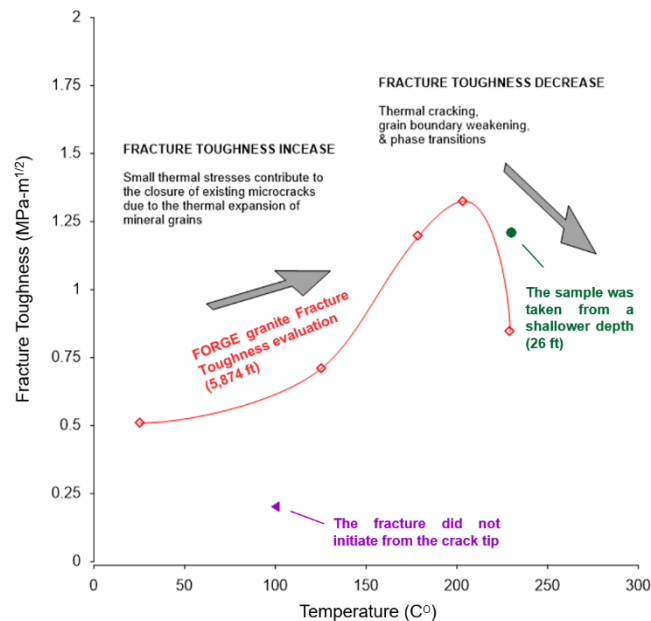


Figure 5: Raw data from experiments conducted by the proposers on Utah FORGE field laboratory samples. The results show a clear trend of increasing fracture toughness, followed by a drop. These data are for granite samples retrieved from a depth of 5,874 ft (red squares and trendline). A shallower granite sample exhibited a fracture toughness value within the expected range (green dot). Notably, in the test conducted at 100°C, the fracture did not initiate at the expected crack tip, and the sample failed at a lower pressure (purple triangle). This suggests failure is likely to occur along a pre-existing natural fracture rather than at the induced crack tip. The fitted red line is based on Equation (7).

Studying temperature-dependent fracture toughness could provide insights into the thermodynamic processes that govern crack growth under extreme conditions. As fracture toughness diminishes with

temperature, the energy required for fracture propagation decreases, implying that geothermal reservoirs may behave more unpredictably as they approach higher temperatures. These thermomechanical interactions require advanced experimental and modeling techniques that account for the non-linear, non-elastic behavior of fracture toughness across a range of temperatures.

Thermomechanical Effects

The absence of detailed experimental data makes it difficult to model the thermomechanical behavior of fractures in high-temperature geothermal systems. Without adequate data, models often rely on simplistic assumptions, such as linear elasticity or ambient-temperature toughness, which may not capture the system's true complexity. In reality, fracture toughness increases with temperature, with sharp reductions near certain thermal thresholds where microcracking and mineral transformations accelerate.

A general form of the non-monotonic relationship between temperature and the fracture toughness at temperature, compared to its value at room temperature (20°C) might be written as:

$$K_{IC}^*(T) = 1 + \frac{A \cdot (T-20)}{1 + e^{B \cdot (T-T_{crit})}} - C \cdot e^{D \cdot (T-T_{crit})} \quad (7)$$

where:

- is the temperature.
- A, B handle the logistic increase for low temperatures.
- C, D control the decay beyond the critical temperature threshold.
- T_{crit} is the critical temperature that marks a transition in the material's fracture toughness behavior

The later (temporally) exponential decay reflects the rapid reduction in fracture toughness observed in some rocks as thermal stress-induced microcracking begins to dominate. Figure 2 shows the fitted curves of the equation above for four rock samples. The fitted parameters are shown in Table 1. However, detailed experimental data across different lithologies are required to accurately determine decay parameters and the temperature ranges where this behavior holds.

Table 1: Fitted parameters for fracture toughness increase and decay measurements from (Hu et al., 2024).

Rock Unit/ Parameter	Increase		Decay	
	A	B	C	D
Iceland Basalt	1.05e-02	7.12e-02	1.50e+02	9.53e-02
Vesuvian Basalt	1.05e-02	7.12e-02	1.50e+02	1.68e-03
Granite (Hu)	3.60e-03	1.46e-02	2.74e+02	2.27e-01
Granite (Wang)	2.01e-03	1.00e-01	2.27e+02	8.79e-02

Complexities of Thermally Induced Damage

Thermal stresses induced by temperature gradients play a major role in fracture propagation, yet comprehensive experimental data on thermally induced damage are sparse. For example, Alneasan et al. (2022) highlight the influence of microcracking induced by thermal treatments, noting that while crack velocity and fracture toughness change with increasing temperature, the detailed effects of thermal cycling and long-term exposure remain poorly understood. Thermal cracking and damage can be modeled

by considering the thermal stress (σ_{th}) *induced* by temperature changes. The thermal stress is related to the temperature change ΔT and the coefficient of thermal expansion of the rock $\sigma_{th} = E \cdot \alpha \cdot \Delta T$. This thermally induced stress can initiate and propagate microcracks, particularly in brittle rocks, and significantly reduce fracture toughness. Still, detailed experimental studies quantifying these effects across various geothermal temperatures are lacking.

6. Conclusions

This report compiles and documents a fracture-toughness dataset for Utah FORGE core material measured using semi-circular bending (SCB) tests, emphasizing at-temperature (“real-time”) testing to reduce bias associated with post-heating cooling protocols. Ambient-temperature measurements from Well 58-32 establish a baseline range of Mode-I fracture toughness across crystalline lithologies and sample orientations.

The at-temperature FORGE granite results show a clear non-monotonic $K_{IC}(T)$ response, characterized by an increase in fracture toughness at moderate temperatures followed by a decrease as temperature approaches and exceeds ~ 200 °C, consistent with the competing effects of microcrack closure at lower temperatures and thermal microcracking and high-temperature weakening mechanisms at higher temperatures.

A key quality-control outcome is that at least one specimen tested at 100 °C did not initiate fracture from the intended notch tip and failed at a lower load, consistent with failure along a pre-existing natural discontinuity; this behavior is explicitly flagged as a validity exception in the dataset.

7. Acknowledgement

We extend our sincere gratitude to Jim Marquardt for his expert assistance in conducting the experiments and to Utah FORGE for providing samples.

8. References

- Alneasan, M., Alzo’ubi, A.K., Behnia, M., Mughieda, O., 2022. Experimental observations on the effect of thermal treatment on the crack speed and mode I and II fracture toughness in brittle and ductile rocks. *Theor. Appl. Fract. Mech.* 121, 103525. <https://doi.org/10.1016/j.tafmec.2022.103525>
- Anderson, T.L., 2017. *Fracture Mechanics*. Taylor & Francis Group.
- Dontsov, E.V., Suarez-Rivera, R., 2020a. Propagation of multiple hydraulic fractures in different regimes. *Int. J. Rock Mech. Min. Sci.* 128, 104270. <https://doi.org/10.1016/j.ijrmms.2020.104270>
- Dontsov, E.V., Suarez-Rivera, R., 2020b. An equivalent representation of multiple hydraulic fractures with a smaller number of fractures for reservoir modeling. *ARMA Am. Rock Mech. Assoc.* ARMA 20-1834.
- Dvory, N.Z., David McLennan, J., Singh, A., James McPherson, B., 2024a. Avoiding the Salts: Strategic Fracture Propagation Management for Enhanced Stimulation Efficiency in the Cane Creek Play, in: *The Unconventional Resources Technology Conference*. Presented at the The Unconventional Resources Technology Conference, American Association of Petroleum Geologists, Houston, TX USA. <https://doi.org/10.15530/urtec-2024-4043632>
- Dvory, N.Z., McLennan, J.D., McPherson, B.J., 2025. Optimizing Hydraulic Fracturing: Managing Fracture Toughness and Stress Shadow Effects in the Paradox Basin. *Rock Mech. Rock Eng.* <https://doi.org/10.1007/s00603-025-04634-1>

- Dvory, N.Z., McLennan, J.D., McPherson, B.J., 2024b. Optimizing Hydraulic Fracturing in the Paradox Formation: A Geomechanical Study of the Cane Creek Play. *Am. Rock Mech. Assoc. ARMA* 24–1158.
- Hu, Yuefei, Hu, Yaoqing, Zhao, G., Jin, P., Zhao, Z., Li, C., 2022a. Experimental Investigation of the Relationships Among P-Wave Velocity, Tensile Strength, and Mode-I Fracture Toughness of Granite After High-Temperature Treatment. *Nat. Resour. Res.* 31, 801–816. <https://doi.org/10.1007/s11053-022-10020-3>
- Hu, Yuefei, Hu, Yaoqing, Zhao, G., Jin, P., Zhao, Z., Li, C., 2022b. Experimental Investigation of the Relationships Among P-Wave Velocity, Tensile Strength, and Mode-I Fracture Toughness of Granite After High-Temperature Treatment. *Nat. Resour. Res.* 31, 801–816. <https://doi.org/10.1007/s11053-022-10020-3>
- Jaeger, J.C., Cook, N.G.W., Zimmerman, R.W., 2007. *Fundamentals of Rock Mechanics*. Blackwell Publishing, Malden, MA.
- Justo, J., Castro, J., Cicero, S., 2020. Notch effect and fracture load predictions of rock beams at different temperatures using the Theory of Critical Distances. *Int. J. Rock Mech. Min. Sci.* 125, 104161. <https://doi.org/10.1016/j.ijrmms.2019.104161>
- Kuruppu, M.D., Obara, Y., Ayatollahi, M.R., Chong, K.P., Funatsu, T., 2014. ISRM-Suggested Method for Determining the Mode I Static Fracture Toughness Using Semi-Circular Bend Specimen. *Rock Mech. Rock Eng.* 47, 267–274. <https://doi.org/10.1007/s00603-013-0422-7>
- Mahanta, B., Singh, T.N., Ranjith, P.G., 2016. Influence of thermal treatment on mode I fracture toughness of certain Indian rocks. *Eng. Geol.* 210, 103–114. <https://doi.org/10.1016/j.enggeo.2016.06.008>
- Sun, Q., Zhang, W., Xue, L., Zhang, Z., Su, T., 2015. Thermal damage pattern and thresholds of granite. *Environ. Earth Sci.* 74, 2341–2349. <https://doi.org/10.1007/s12665-015-4234-9>
- Timoshenko, S., Goodier, J.N., 1970. *Theory of elasticity*.
- Wang, P., Wang, G., Wang, C., Jiang, Y., 2025. Fracture mechanisms of granite subjected to varied thermal treatments: Insights into cooling-induced failure characteristics. *Theor. Appl. Fract. Mech.* 138, 104942. <https://doi.org/10.1016/j.tafmec.2025.104942>
- Yin, T., Li, X., Xia, K., Huang, S., 2012. Effect of Thermal Treatment on the Dynamic Fracture Toughness of Laurentian Granite. *Rock Mech. Rock Eng.* 45, 1087–1094. <https://doi.org/10.1007/s00603-012-0240-3>
- Yin, T., Wu, Y., Li, Q., Wang, C., Wu, B., 2020. Determination of double-K fracture toughness parameters of thermally treated granite using notched semi-circular bending specimen. *Eng. Fract. Mech.* 226, 106865. <https://doi.org/10.1016/j.engfracmech.2019.106865>